HEFAT2008
6th International Conference on Heat Transfer, Fluid Mechanics and Thermodynamics
30 June to 2 July 2008
Pretoria, South Africa
Paper number: CC1

INFLUENCES OF WETTING CONDITION TO ROSENSWEIG INSTABILITY OF A FERROFLUID DROPLET

Ching-Yao Chen[1,*], Z.-Y. Cheng[2], C.-Y. Hong[3]
[1]Department of Mechanical Engineering, National Chiao Tung University, Taiwan
[2]Department of Mechanical Engineering, National Yunlin University of Science and Technology, Taiwan
[3]Department of Mechanical Engineering, Nan-Kai Institute of Technology, Taiwan
*Corresponding Author: chingyao@mail.nctu.edu.tw

ABSTRACT
Experiments are carried to investigate the interfacial morphologies of a thin film of micro magnetic drops under a constant perpendicular field. Strong dependences of the drop breakup patterns on their initial sizes and wetting conditions are observed. Three modes of well-ordered breakup instability patterns are identified for drop sizes ranged from D≈800μm to 2,200μm for a field strength of H=346Oe on a dry plate. The pattern of breaking sub-scale droplets can be categorized into three main parts: (1) a central droplet, (2) the outer fluids in forms of either an outer residual annulus or an outer array of primary subdroplets, and (3) the middle region that might evolve into a single circular array of middle subdroplets. A more complex and disorder mode IV instability is recorded for large drop sizes D≥2,300μm. Nevertheless, the central droplet is pulled apart for an even large droplet D≥2,600μm, and is referred as a new mode V instability although the topology remains features of the mode IV instability. Because of height variation along the ferrofluid surface, domination of the central droplet is significant. On the other hand, a prewetted plate leads to a nearly flat fluid surface. The breakups of sub-scale droplets are nearly evenly distributed. The sizes sub-scale droplets are weakly dependent on their initial diameters. The number of breaking sub-scale droplets N and the diameter of initial droplet D can be approximated by a correlation of $N \sim D^2$.

INTRODUCTION
Since the early 1960s, magnetic fluids (ferrofluids) have been synthesized for technical applications [1]. The magnetic fluids consist of layers of surfactants coated on nano magnetic particles to form colloidal suspensions in carrier fluids such as water and oil. Controlled by an external magnetic field, the magnetic fluids have been successfully applied on wide scopes of engineering applications, such as rotary feeds in hard disc drives and speakers [2]. In addition, practical uses in biomedicine [3] have been achieved because of the great success in the development of stable ferro colloids during the last decade. On the other hand, the interfacial instabilities of magnetic fluids under a static perpendicular field also interest researchers from both scientific and practical points of views. Two main branches of the interfacial instability issues are investigated intensively, namely, the labyrinthine instability [4] and the Rosensweig instability [5]. An intricately patterned instability (labyrinthine instability) is reported by Romankiw et al. [4], if the fluid is contained between two close spaced plates (Hele–Shaw cell) and subjected to a normal field. Since then, great efforts have been devoted to this branch of interfacial instability. Detailed mechanisms of labyrinthine instabilities on the immiscible interfaces are addressed by [6–13], such as effects of the dimensionless magnetic Bond number $Bm \equiv 2M^2h/\sigma$ that characterizes the ratio of the magnetic force to the surface tension, and the dimensionless diameter $P \equiv d/h$, which is the ratio of droplet diameter d to cell gap width h. The notations of M and σ represent the magnetization and the surface tension of the magnetic fluid against the surrounding fluid such as air in the conventional studies. As to the situations of miscible interface [14–16], they involve an additional effect of diffusion. The interfacial instability on the free surface of a horizontal magnetic layer, which is not confined on the top, is firstly studied by Cowley and Rosensweig [5]. If the magnetic strength exceeds a critical magnetic Bond number, a sudden transition from an original flat surface into a hexagonal pattern of three-dimensional liquid crests, or the so-called Rosensweig crests, is observed. The patterns of Rosensweig crests are experimentally demonstrated by means of radioscopy [17, 18]. Berkovsky and Bashtovoi [19] conducted experiments in an extremely thin film and observed the phenomenon of rupture of continuity with individual droplets that preserve the hexagonal geometry.

In addition, the pinch-off of a magnetic liquid bridge was observed by Richter et al. [18]. Moreover, intensive studies have also been conducted on the dynamics of crests experimentally [20–24] and theoretically [25]. Nevertheless, these researches focus mainly on the magnetic fluid layer at a relative larger scale. With the advances in micro-technologies, it is interesting to further investigate the instability phenomena of an extremely thin film, which is strongly affected by the surface tension.

Recently, Chen and Lo [26,27] studied a droplet of thin film with diameters ranging from $O(10^2 \sim 10^3)$ μm, under an instant perpendicular field on a dry plate. The droplet is observed to breakup into numerous sub-scale droplets depending on its initial diameter. This particularly simple phenomenon can be possibly applied as a non-invasive mean for partition of micro-scale droplets. Four interesting modes of film ruptures were observed if the field strength is kept constant. Nevertheless, the topologies of ruptures are solely discussed by the top views, in which the very important third dimensional effects of Rosensweig crests can not be fully understood. In the present investigation, besides the images from top views we also record the side views that are able to give comprehensive explanations for the film rupture mechanism. In addition, similar experiments are carried out for situations in a prewetted conditions to resolve the unevenly formation of sub-scale droplets on a dry plate.

The experimental setup consists of a circular thin film of micro magnetic drop placed on a glass plate subjected to a perpendicular field, as shown in Fig. 1. The magnetic fluid used is a light mineral oil-based ferrofluid (EMG901) produced by the Ferrotec Corp. The magnetic response is given by a Langevin function [1] with the saturation magnetization Ms = 660 gauss. The field strength is generated by a pair of coils in the Helmholtz configuration powered by a programmable power source. The power source is turned on instantly to the desired strength to H=346Oe and kept constant by fixed the current strength. We record the interfacial morphologies of the ferrodrop by a charge-coupled device (CCD) camera. The images are used to analyze both qualitatively and quantitatively.

RESULTS AND DISCUSSION

Qualitative Observations: Cases on a Dry Plate Surface

We first describe the observation of a representative case for a magnetic drop of initial diameter D≈900μm, as the images of top and side views at the initial and equilibrium states shown in figure 2. It should be noticed that, because of reflection only the right half (slightly darker) parts of side views shown in figure 2 represent the actual images of ferrodroplet. The initial image of side view appears a typical hydrophilic film of a maximum height estimated as h≈43μm. Similar to the findings reported in Ref.[26,27], the magnetized drop subjects an instant third dimensional upward force when the perpendicular field is turned on. This upward force tends to lift the drop, and consequently pulls the circumference toward the center. However, the surface tension tends to resist this sudden inward pulling effect. As a result, the drop is broken up into numerous sub-scale droplets, including a largest "central droplet" near the original drop's center surrounded by a circular array that consists of 7 smaller and nearly evenly distributed "subdroplets", as shown in the top view of figure 2 which is referred as to the mode II instability in Ref.[26]. The diameters of central droplet and subdroplets are measured at D_c≈189μm and D_s≈122μm, respectively. According the topology observed in figure 2, the total number of breaking sub-scale droplets, denoted as N, can be counted as N=8 in the present case. This particular number can be used to determine the prominence of droplet breakup instability. More detailed transient morphological evolutions are referred to Ref.[26]. It is noteworthy that the "sub-scale droplets" observed from top views are not plain two-dimensional circular films but typical three-dimensional Rosensweig crests with sharp spikes as shown by the side views in figure 2. These third dimensional structures explain the decrease of total area occupied by the magnetic fluid. Nevertheless, in order to be consistent with the top circular morphology, we simply refer them as "droplets". The correspondent side view of the ruptured droplet clearly demonstrates domination of the central droplet (the highest central Rosensweig crest). The height of central droplet (h_c≈311μm) is much larger than those outer subdroplets (or outer lower Rosensweig crests) whose heights are nearly identical (h_s≈108μm). The volume of individual droplet is approximated by the formulation of a circular cones, i.e. $V=hD^2/12$. The volume ratio (R_v), defined as $R_v \equiv V_c / V_s$, where V_c and V_s denote the volumes of central droplet (or central Rosensweig crest) and individual subdroplet (or outer Rosensweig crest) respectively, can be used to determine the dominance of central droplet and is estimated as R_v ≈7.5 in the present representative case. The dominance of central droplet ($R_v >> 1$) is attributed to various initial heights of the fluid film. The predominance of original height at the central region naturally leads to a minimum curvature along the field (vertical) direction. On the other hand, maximum curvatures are resulted from lower surface heights near the contact region. As a result, stronger constraints of surface tension are induced near the contact region, and weaker at the central area. The weak constraint of surface tension near the center allows a major surface deformation and results to a formation of dominant central droplet. We like to point out the dominance of a central droplet is a disadvantage if even breakups of sub-scale droplets are desired for further applications. A unity value of volume ration, i. e. R_v =1, is the optimal situation for the formation of sub-scale droplets.

We now consider the situations of ferrodroplets with various initial diameters. For a smaller droplet of

D≈800 μm, as shown in figure 3, the breakup of ferrodrop shows a different pattern. While the formation of a central droplet is still similar to the previous representative case, a "fluid annulus", instead of a circular array of subdroplets, is observed to surround the central droplet as shown in figure 3, which is referred as to the mode I instability [26]. The diameter of central droplet is measured at about D_c≈214μm. The side view shown in figure 3 clearly demonstrates a dominant central droplet (h_c≈548μm) associated with a lower height of annulus of slightly waving surface. Without the formation of any separated subdroplets, no volume ratio can be defined in the present smaller droplet. The formation of single central droplet (N=1) indicates a more stable situation regarding the droplet breakup. The reason for current more stable situation can be explained by the overall larger fluid surface curvatures as shown in figure 3. For a smaller droplet, the smaller spread area of fluid associated with a constant contact angle, which is an intensive fluid property, would lead to lower initial heights along the fluid surface. Consequently, that the vertical curvatures and their induced constraints of surface tension would be stronger than the previous case of a larger diameter. As a result, the breakup instability of ferrodroplet would be milder.

On the other hand, if the size of drop is slightly increased to D≈1,200μm, the breakup instability is enhanced as the images shown in figure 4. By the same reason stated above, as the total surface area increases for a larger droplet under a constant contact angle, heights on of the fluid surface are larger compared to the previous cases of smaller droplets. This allows larger area of surface with weaker constraints of surface tension to evolve into droplet breakup, so that the instability is enhanced in a larger droplet. While the pattern of droplet breakup remains similar to the representative case of D≈900μm, i.e. the mode II instability, the number of distinguishable subdroplets on the outer circular array increases slightly to 8 as appeared in figures 4. Even those subdroplets might still seem not formed separately by the top view, the side view clearly demonstrates their fully evolutions to individual subdroplets, and resulted in a total number of breaking sub-scale droplets N=9. In addition, dominance of the central droplet is still preserved. The volume ratio increases further to R_v≈11.3 in the present situation. Similar results are also obtained for a droplet of diameter D≈1,400μm as sown in figure 5. If the drop's diameter is further increased to D≈1,600μm, as shown in figure 6, the breakup phenomena are seen more vigorous. Besides the previously observed central droplet and many subdroplets at the outer array, an additional circular array of droplets is formed in the middle region, referred as to "middle subdroplets" herein. In addition, smaller "secondary subdroplets" appear at the intervals of subdroplets at the outer array. This more vigorous and new instability pattern is referred as to the state of "mode III" instability [26]. The total distinguishable sub-scale droplets, counted from the top view in figure 6, is about N=19. Nevertheless, the 3-dimensional structures of these additional subdroplets, i.e. the heights of middle and secondary subdorplets, are not that significant as shown in figure 6. The breaking sub-scale droplets are still dominated by the previously described central droplet and main subdroplets. As a result, the parameter of volume ratio R_v can be still applied to determine the dominance of central droplet. A even larger R_v ≈12.2 is measured. The droplet breakup instability for an even larger drop of initial diameter up to D≈2,500μm shows extremely vigorous breakups of numerous sub-scale droplets, referred as to the mode IV instability [26]. The droplet pattern appears more complex with multi circular arrays of middle subdroplets. Nevertheless, for a droplet is significantly large (D≥2,600μm), as a typical situation of D≈2,600μm shown in figure 7, even the main topology of top view retains the main features of mode IV instability described above, very large volume of the central droplet is pulled apart from the plate as the snapshot image shown in figure 7. As we discussed earlier, constraint of surface tension is further weakened in the present significant large surface area, and no longer able to sustain the magnetic upward lift. Consequently, a major portion of central droplet fluid is pulled away. The residual central droplet is smaller than subdroplets as shown in figure 7. The image of side view clearly shows the significant mass loss of central droplet. Under this situation, volume ratio is not meaningful (or R_v<1). As a result, the applicability of current method to generate sub-scale droplets is limited by a maximum diameter. We referred this limit of mass loss of central droplet as to the new mode V instability.

Qualitative Observations: Cases on a Prewetted Plate Surface

According to the results on a dry plate discussed above, it can be concluded that the local height (or vertical curvature) of fluid surface is crucial to the formation of different patterns of instability. Under the situation of a smaller droplet, the effect of constant contact angle gives lower heights (curvatures) along the fluid surface. The lower surface heights lead to stronger constraints along the surface, and results to not just more stable instability reflected by less numbers of breaking sub-scale droplets, but also a less dominant central droplet. On the other hand, a larger initial droplet provides more area of relatively weaker surface constraints and allows the formation of more number of sub-scale droplets. As a result, modifications of wetting conditions on the plate, which would lead to a different contact angle, are natural means to manipulate the patterns of instability. In this section, we present the similar experiments on a plate prewetted by the mineral oil solvent of ferrofluid. A correspondent case of D≈900μm, which should be compared to the representative case in figure 2, is shown in figure 8. The modification of contact surface immediately reduces the contact angle dramatically. A nearly flat fluid surface of

extremely thin film is formed as displayed in the side view of figure 8. This thin and nearly flat surface results to a nearly uniformed and weak constraint of surface tension, so that a greater number of breaking sub-scale droplets (N=19) is generated as shown in figure 8. In addition, the dominance of central droplet is no longer observed with all the sub-scale droplets appear near a unique size and height (or $R_v \approx 1$). This pattern of nearly uniform breakup is nicely preserved even for various initial sizes as shown in figure 9. For all the sizes experimented, although a greater number of sub-scale droplets is generated for a larger droplet as expected, the size of individual sub-scale droplet, represented by the diameter D_p, remains quite close even among different initial diameters, i.e. $D_p \approx 195 \pm 40\mu m$. A more quantitative confirmation for a unique size of sub-scale droplets among various diameters will be provided later. The reason for formation of subdroplets with a global size is because of the almost flat fluid interfaces. Unlike the cases on a dry plate, the heights of local fluid surface varies due to the significant contact angle, nearly flat surfaces are formed in the current prewetted condition regardless the initial diameters. As a result, sub-scale droplets with a global size are generated without apparent influences of initial diameter of original droplet.

Quantitative Analysis: Number and Volume of Breaking Sub-scale Droplets

We conclude the results by plotting the numbers of all distinguishable sub-scale droplets N, including the central droplet, subdroplets, middle subdroplets and secondary subdroplets, as well as the volumes of central droplet (V_c) and subdroplets (V_s) at various initial diameters D. Shown in figure 10 is the mean number of sub-scale droplets (N) at various initial droplet's diameters (D) for both dry and prewetted conditions. For the situation on a dry plate, while the numbers of sub-scale droplets increase with the initial diameter, apparent sudden jumps, which indicate the mode changes, are observed. Consistent with early study [26], four major ranges, i.e. $D \leq 900\mu m$, $1,000\mu m \leq D \leq 1,400\mu m$, $1,400\mu m \leq D \leq 2,300\mu m$ and $D \geq 2,300\mu m$, which correspond to four modes of instability [26]. Nevertheless, we like to point out again that significant mass lost occurs for $D > 2,600\mu m$ due to the pulling apart of central droplet, referred as to mode V instability, even the quantitative trend of sub-scale droplets is similar to the mode IV instability. In general, no certain numerical correlation is found to describe the dependence of N and D under the situation on a dry plate. Volumes of individual sub-scale droplets shown in figure 11 clearly demonstrate the significant dominance of central droplet. While the volumes of subdroplets (V_s) generally appear to increase with the initial size (D) monotonically, the increment is not that significant. It is attributed to the fact of constant contact angle. Since sizes of these outer subdroplets are affected by the local heights of fluid surface which are influenced greatly by contact angle. As a result, the variation would not be too significant under a constant contact angle. Nevertheless, the volumes of central droplet appear more dramatic variation as the increase of the initial diameter. For the cases of mode I, II and III ($D < 2,300\mu m$), larger volumes of the central droplet are observed for bigger initial diameters. Unlike subdroplets which are mainly affected by the constant contact angle, formation of the central droplets is determined by the maximum surface height in the middle region. As explained previously, a larger spread area associated with constant contact angle leads to a greater height. Consequently, the volumes of central droplet would be significantly greater for a larger initial droplet. However, volumes of the central droplets start to reduce if the initial size is further increased for $D \geq 2,300\mu m$, where the mode IV instability evolves. The volume reduction is caused by the formation of numerous middle subdroplets, which share significant part of fluid in the middle region. In final words, even a greater number of sub-scale droplets is generated by a larger initial droplet, significant volume unbalance always exists among these sub-scale droplets. On the other hand, the number of breaking sub-scale droplets on a prewetted plate appears a gradual increase as the initial droplets are enlarged, as also shown in figure 10. No dramatic mode transition occurs in the present cases on a prewetted plate. In addition, the correlation can be approximated by a proportionality of $N \sim D^2$. This proportionality further quantitatively confirms the global diameter of all sub-scale droplets regardless their initial sizes, so that the breakups are more evenly formed.

CONCLUSIONS

We present the experiments to investigate the interfacial morphologies of a thin film of micro magnetic drops under a constant perpendicular field. Experimental results demonstrate the breakup of the initial droplet into numerous sub-scale droplets. We have shown a strong dependence of the breakup patterns on the initial sizes and wetting condition. Consistent with the previous study [26], three modes of well-ordered patterns of breakup instability are identified for sizes ranged from $D \approx 800\mu m$ to $2,200\mu m$ for the field strength H=346Oe on a dry plate. The pattern structures can be categorized into three main parts: (1) a central droplet, (2) the outer fluids in forms of either an outer residual annulus/ring or an outer array of primary subdroplets with/without secondary subdroplets, and (3) the middle region that might evolve into a single middle array of middle subdroplets. A more complex and disorder mode IV instability is recorded for large drop sizes $D \geq 2,300\mu m$. Nevertheless, the central droplet is pulled apart for an even large droplet $D \geq 2,600\mu m$, and is referred as a new mode V instability even the topology remains the features of mode IV instability. Because of height variation along the ferrofluid surface, domination of the central droplet is observed. The volume of central droplet increases as the initial diameter until the mode IV pattern is formed. The mass loss occurs in the mode V

region as well as the unevenly breakups of sub-scale droplets are disadvantages if partition of the droplets for further applications is desired. On the other hand, a plate prewetted by mineral oil leads to a nearly flat fluid surface. The breakups of sub-scale droplets are nearly evenly distributed. In addition, the sizes of sub-scale droplets are weakly dependent on their initial diameter. The number of breaking sub-scale droplets N and the diameter of initial droplet D can be approximated by a correlation of $N \sim D^2$.

ACKNOWLEDGEMENTS

This research is supported by the National Science Council of the Republic of China through the grant NSC 95-2221-E-009-369-MY3.

REFERENCES

[1] R. E. Rosensweig.Ferrohydrodynamics (Cambridge University Press, New York, 1985).

[2] B. M. Berkovsky, V. Bashtovoi . Magnetic Fluids and Applications Handbook (Begell House Inc., New York, 1996).

[3] Q. Pankhurst, J. Connolly, S. Jones, J. Dobson. Applications of magnetic nanoparticles in biomedicine. J. Phys. D: Appl. Phys., vol. 36 (2003), pp. R167–R181.

[4] L. Romankiw, M. Slusarczak, D. Thompson. Liquid magnetic bubbles. IEEE Trans. Magnetics, vol. MAG-11 (1975), pp. R25–28.

[5] M. D. Cowley, R. E. Rosensweig. The interfacial stability of a ferromagnetic fluid. J. Fluid Mech., vol. 30 (1967), pp. 671–688.

[6] A. Cebers, M. M. Maiorov. Magnetostatic instabilities in plane layers of magnetizable liquids . Magnetohydrodynamics , vol. 16 (1980), no. 1, pp. 21–27.

[7] A. Cebers, M. M. Maiorov. Structures of interface of a bubble and magnetic fluid in a field . Magnetohydrodynamics , vol. 16 (1980), no. 3, pp. 231–235.

[8] S. A. Langer, R. E. Goldstein, D. P. Jackson. Dynamics of labyrinthine pattern formation in magnetic fluids. Phys. Rev. A., vol. 46 (1992), no. 8, pp. 4894–4904.

[9] Dickstein, S. Erramilli, R. Goldstein, D. Jackson, S. Langer . Labyrinthine pattern formation in magnetic fluids . Science , vol. 261 (1993), pp. 360–365.

[10] D. Jackson, R. Goldstein, A. Cebers . Hydrodynamics of fingering instabilities in dipolar fluids . Phys. Rev. E. , vol. 50 (1994), no. 1, pp. 298–307.

[11] I. Drikis, A. Cebers . Viscous fingering in magnetic fluids: numerical simulation of radial Hele-Shaw flow . J. Magn. Magn. Mater , vol. 201 (1999), pp. 339–342.

[12] A. Cebers, I. Drikis . Labyrinthine Pattern Formation in Magnetic Liquids, Free Boundary Problems: Theory and Applications (Chapman and Hall/CRC, edited by Athanasopoulos et. al, 1998).

[13] C. Flament, G. Pacitto, J. Bacri, I. Drikis, A. Cebers . Viscous fingering in a magnetic fluid. I. Radial Hele-Shaw flow . Phys. Fluids , vol. 1 (1998), pp. 2462–2472.

[14] C.-Y. Chen . Numerical simulations of fingering instabilities in miscible magnetic fluids in a Hele-Shaw cell and the effects of Korteweg stresses . Phys. Fluids , vol. 15 (2003), no. 4, pp. 1086–1089.

[15] A. Igonin, A. Cebers . Labyrinthine Instability of miscible magnetic fluids . Phys. Fluids , vol. 15 (2003), no. 6, pp. 1734–1744.

[16] C.-Y. Chen, H.-J. Wu . Numerical simulations of interfacial instabilities on a rotating miscible magnetic droplet with effects of Korteweg stresses. Phys. Fluids , vol. 17 (2005), no. 4, 04210 pp. 1–8.

[17] R. Richter, J. Blasing . Measuring surface deformations in magnetic fluids by radioscopy. Rev. Sci. Instrum., vol. 72 (2001), pp. 1729–1733.

[18] R. Richter, B. Reimann, A. Lange, P. Rupp, A. Rothert . Magnetic liquid patterns in space and time. Advanced in Solid State Physics, vol. 43 (2003), pp. 789–800.

[19] B. M. Berkovsky, V. Bashtovoi . Instabilities of magnetic fluids leading to a rupture of continuity. IEEE Trans. Magnetics , vol. MAG-16 (1980),pp. 288–297.

[20] M. Ohaba, J. Sudo . Liquid surface behavior of a magnetic liquid in a container subjected to magnetic field and vertical vibration . J. Magn. Magn. Mater. , vol. 149 (1995), pp. 38–41.

[21] F. Elias, C. Flament, J.-C. Bacri . Motion of an asymmetric ferrofluid drop under a homogeneous time-dependent magnetic field . Phys. Rev. Lett., vol. 77 (1996), pp. 643–646.

[22] R. Rosensweig, S. Elborai, S.-H. Lee, M. Zahn . Ferrofluid meniscus in a horizontal or vertical magnetic field. J. Magn. Magn. Mater., vol. 289 (2005), pp. 192–195.

[23] M.Zahn. Magnetic fluids and nanopractical applications to nanotechnology. J. Nanopart. Res., vol. 3 (2001), pp. 73–78.

[24] R. Richter, I.V. Barashenkov. Two-dimensional solitons on the surface of magnetic fluids. Phys. Rev. Lett., vol. 94 (2005), 184503, pp. 1–4.

[25] A. Lange, H. Langer, A. Engel. Dynamics of a single peak of the Rosensweig instability in a magnetic fluid . Physica D , vol. 140 (2000), pp. 294–305.

[26] C.-Y. Chen, L.-W. Lo. Breakup of thin films of micro magnetic drops in perpendicular fields. J. Magn. Magn. Mater. , vol. 305(2006), 2, pp. 440-447.

[27] C.-Y. Chen, C.-H. Chen, L.-W. Lo., Breakup and Separation of Micro Magnetic Droplets in a Perpendicular Field, J. Magn. Magn. Mater., vol.

310(2007), 2P3, pp. 2832-2834.

Figures:

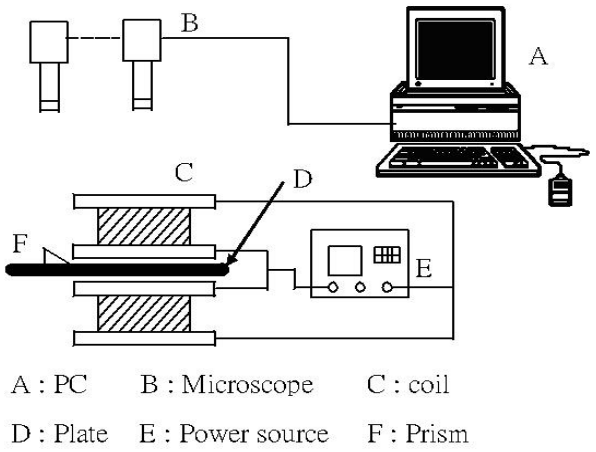

Fig. 1: Principle sketch of experimental setup: the experimental setup consists of a thin film of micro magnetic drop placed on a glass plate subjected to a perpendicular field. The field strength is provided by a pair of coils in the Helmholtz configuration powered by a computerized programmable power source. The images of top and side (via reflection of the prism) views are recorded by a CCD camera.

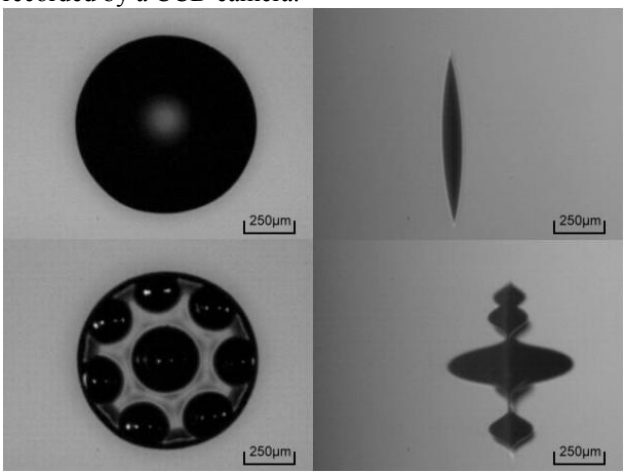

Fig. 2: Snap-shots for a representative case: diameter of the initial drop D≈900 μm. Shown in the top row are the top (left) and side (right) views in original state. Because of reflection, only the right half (slightly darker) part of the side view image is the real shape of ferrofluid droplet. A mode II instability which consists of a dominant "central droplet" with an outer circular array of 7 "subdroplets" is observed under the influences of magnetic field, as the top (left) and side (right) views in the bottom row. The total number of breaking sub-scale droplets is N=8.

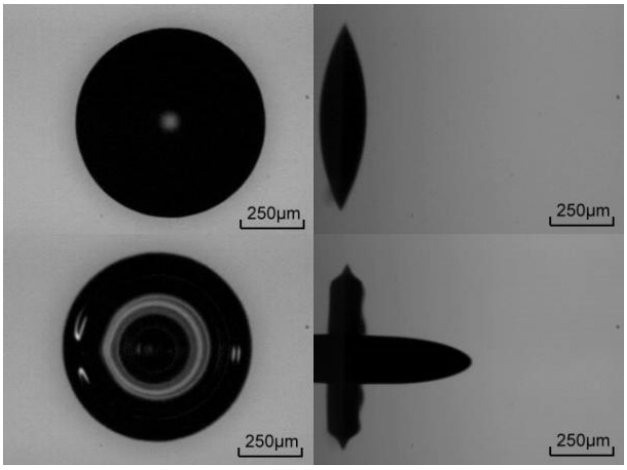

Fig 3: Mode I instability for an initial drop D≈800 μm: the drop is ruptured into a central droplet surrounded by a fluid annulus.

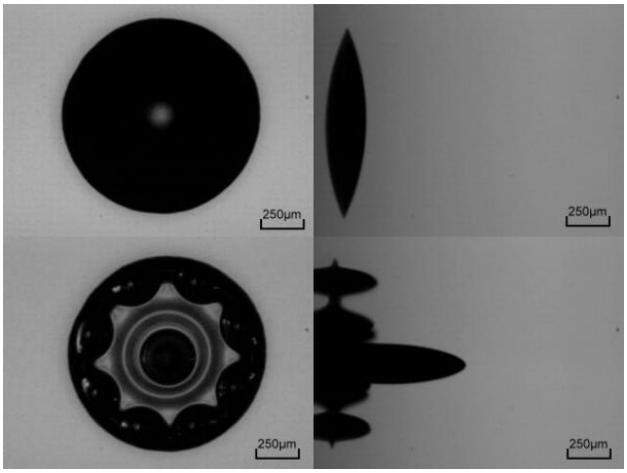

Fig. 4: A mode II instability is observed for D≈1,200 μm. A higher number of breaking sub-scales droplets (N=9) indicates a more vigorous instability.

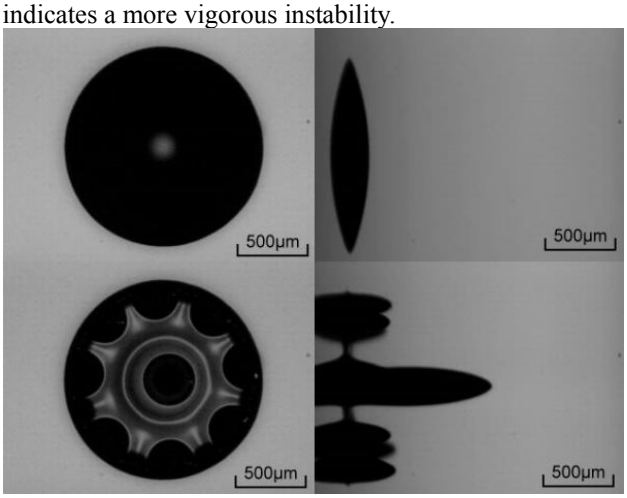

Fig. 5: A mode II instability is observed for D≈1,400 μm.

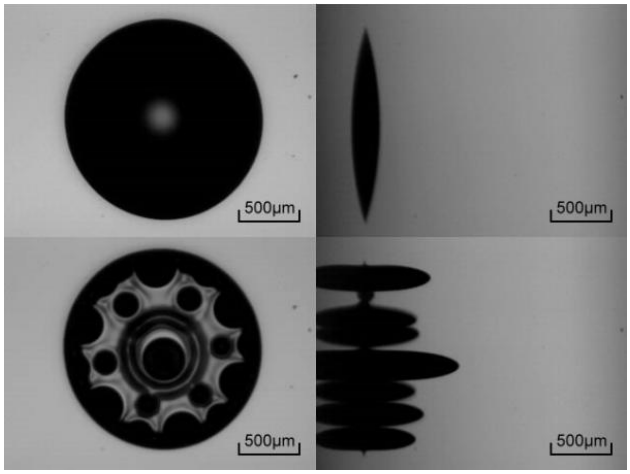

Fig. 6: Images for an initial drop D≈1,600 μm: a more vigorous mode III instability with an additional circular array of "middle subdroplets" in the middle region and numerous smaller "secondary subdroplets" in the outer array is observed.

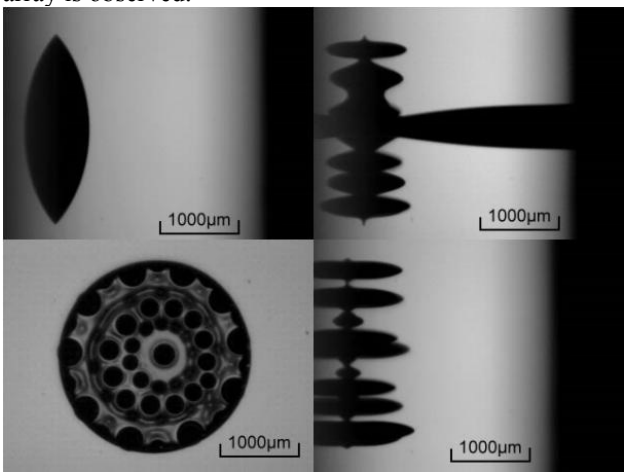

Fig. 7: 2 Snap-shots for an initial drop D≈2,600 μm: even the images in equilibrium state (bottom row) remains the features of mode IV instability, the central droplet is pulled apart (snap-shot image in upper right) which is referred as to a new phenomenon of mode V instability.

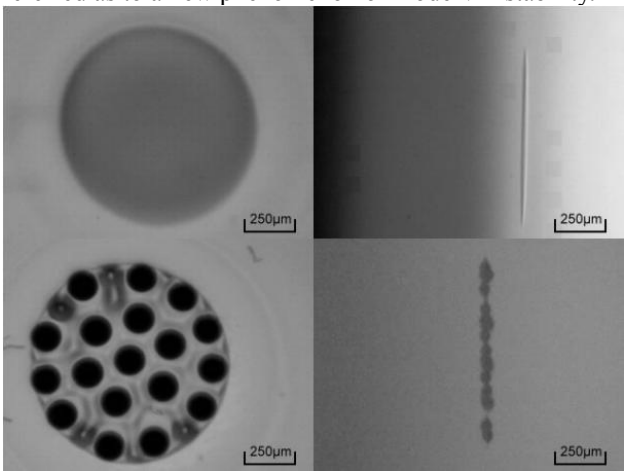

Fig. 8: A droplet of D≈900μm on a prewetted plate: a nearly flat surface (upper right image) results to a greater number of breaking sub-scale droplets (N=19, lower left image). In addition, the dominance of central droplet is no longer observed with all the sub-scale droplets appear nearly a unique size and height (bottom images).

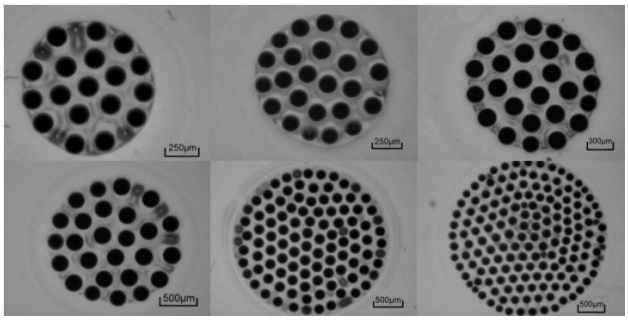

Fig. 9: The pattern of nearly uniform breakup on a prewetted plate is nicely preserved for various initial sizes.

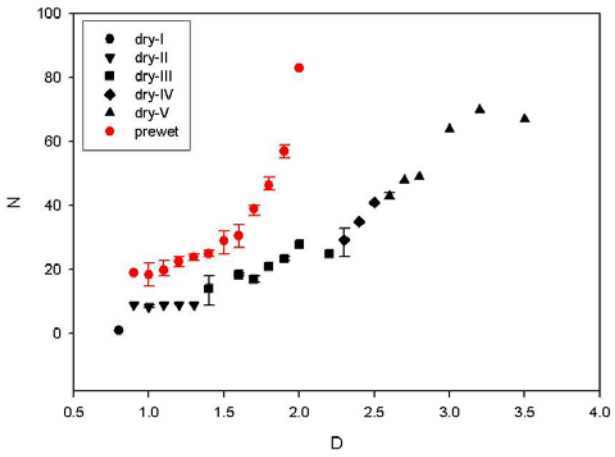

Fig. 10: Numbers of breaking sub-scale droplets N vs. original drop diameters D(in mm). The plot clearly shows sudden jumps near the critical diameters for cases on a dry plate which lead to different modes of rupture patterns. On the other hand, the correlation can be approximated by a proportionality of $N \sim D^2$. No dramatic mode transition occurs in the cases on a prewetted plate.

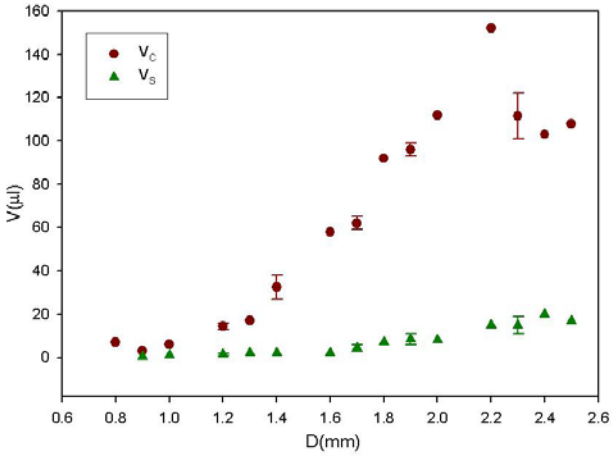

Fig. 11: Volumes of individual sub-scale droplets versus various initial diameters. Significant volume dominance of the central droplet (V_c) is clearly observed against the subdroplets (V_s).